J Solid State Electrochem (2016) 20:1845–1854
DOI 10.1007/s10008-015-3073-7

ORIGINAL PAPER

# Studies on solid-state polymer composite electrolyte of nano-silica/hyperbranched poly(amine-ester)

**Xianlei Hu[1,2] · Gaoming Hou[1] · Mingqiu Zhang[1] · Ruoxin Zhang[2] · Wenhong Ruan[1] · Yifu Huang[1]**

Received: 27 June 2015 / Revised: 27 October 2015 / Accepted: 2 November 2015 / Published online: 27 November 2015


**Abstract** A new solid-state polymer composite electrolyte based on hypergrafted nano-silica ($SiO_2$-g-HBPAE)/hyperbranched poly (amine-ester) (HBPAE) doped with lithium perchlorate ($LiClO_4$) was studied in this paper. The *N*,*N*-diethylol-3-amine-2-methyl methylpropionate monomer was firstly synthesized by methyl methacrylate (MMA) and diethanolamine through Michael addition reaction and then self-condensed on the surface of nano-silica pretreated by 3-aminopropyltriethoxysilane (APTES) and MMA. The synthetic procedure of the monomers and $SiO_2$-g-HBPAE/HBPAE was traced by fluorescence spectra. The size and grafting ratio of $SiO_2$-g-HBPAE were characterized by transmission electron microscopy, static light scattering and thermogravimetric analysis. Incorporating $SiO_2$-g-HBPAE to HBPAE could not only decrease the glass transition temperature of polymer according to the differential scanning calorimetry characterization, but also increase the elastic and viscosity modules indicated by rheological measurement results. Electrochemical properties of $SiO_2$-g-HBPAE/HBPAE/$LiClO_4$ were also investigated. The conductivity of $SiO_2$-g-HBPAE/HBPAE with 50 wt% $LiClO_4$ reached $1.4\times10^{-5}$ S/cm at 30 °C and $10^{-3}$ S/cm at 100 °C. The lithium-ion transference number of synthesized hyperbranched electrolyte can be up to 0.55.

**Keywords** Hyperbranched poly (amine-ester) · Hypergrafted nano-silica · Polymer composite electrolyte · Conductivity · Lithium battery

## Introduction

The conventional lithium-ion battery suffers from evaporation and leakage of the liquid electrolyte during the long-term operation, which leads to the decay of the cell performance and security. In order to improve the long-term stability and security, one way is to develop polymer lithium batteries with solid-state polymer electrolytes to substitute for the traditional volatile liquid electrolytes. This kind of battery is regarded as the most promising rechargeable chemical power source because of its outstanding properties such as high energy density, long cycle life, low leakage, light weight and flexible shape. Thus, extensive researches into polymer electrolyte are being pursued on [1–6]. As known, the primary solid phase polymer electrolytes are poly (ethylene oxide) doped with lithium salts systems, which offer very low ionic conductivity at ambient temperature [7].

Lithium ions have been demonstrated to mainly transport in amorphous regions of polymer electrolyte. So reducing crystallinity of the polymer and increasing mobility of the polymer chains are effective methods to improve the conductivity. Based on this principle, a lot of research has been done via blending [8–11], copolymerization [12–16] and crosslinking [17, 18] to prepare polymer electrolyte systems with less crystallinity, lower glass transition temperature and more segment movement capability. Hyperbranched polymer

Xianlei Hu and Yifu Huang contributed equally to this work.

**Electronic supplementary material** The online version of this article (doi:10.1007/s10008-015-3073-7) contains supplementary material, which is available to authorized users.

✉ Wenhong Ruan
cesrwh@mail.sysu.edu.cn

[1] Key Laboratory for Polymeric Composite and Functional Materials of Ministry of Education of China, GDHPPC Lab, School of Chemistry and Chemical Engineering, Sun Yat-sen University, Guangzhou 510275, China

[2] Guangzhou Tinci Materials Technology Co., Ltd, Guangzhou 510760, China

is one kind of macromolecule with non-crystalline structure, less chain entanglement and plenty of terminal functional groups. At the same time, hyperbranched polymer provides lots of cavities between highly branched structural units. Based on this typical structure feature, hyperbranched polymer not only promotes the dissociation of lithium salts but also provides sufficient segment movement to insure ionic conductivity. So it can be considered as a potential candidate for the polymer electrolyte. Hyperbranched polyether [19, 20], hyperbranched polyester [21, 22] and hyperbranched polyurethane [23–25] have been intensively studied as polymer electrolytes in the past years. But the poor ionic conductivity at room temperature could not satisfy the need for real application in lithium batteries. Pan synthesized an organic-inorganic hybrid polymer electrolyte from γ-glycidoxypropyl trimethoxy silane, cyanuric chloride and a polyether amine for the first time. The conductivity was up to $4.4\times10^{-5}$ S/cm at 30 °C after blending with $LiClO_4$ [26]. This finding opens up a new direction for hyperbranched polymer electrolytes.

It has been well confirmed that the addition of ceramic fillers improves the conductivity of polymer hosts and their interfacial properties in contact with the lithium electrode [27]. The effects of filler species, filler size and filler content on the composite polymer electrolyte were mostly studied [28–30]. It was found that the size of the filler played an important role in improving ionic conductivity. The nano-scale particles exhibit better improvement than micro-scale ones due to the nanometer size effects. Meanwhile, hyperbranched polymer is considered with poor mechanical properties owing to lack of chain entanglement, which limits its application in polymer electrolyte membranes. Previous studies have shown that incorporating inorganic nano-filler to polymer electrolyte is beneficial not only to ionic conduction but also to mechanical properties [31].

Therefore, in the present investigation, $AB_2$ type monomer was synthesized through Michael addition reaction and then self-condensation on the surface of nano-silica pretreated by 3-aminopropyltriethoxysilan (APTES) and methyl methacrylate (MMA) to fabricate solid-state polymer host. During the polycondensation process, hyperbranched poly (amine-ester) (HBPAE) and the hypergrafted nano-silica ($SiO_2$-g-HBPAE) were simultaneously prepared and blended. A series of composite polymer electrolytes were prepared via changing the dosage of hypergrafted nano-silica and lithium perchlorate, denoted as ($SiO_2$-g-HBPAE/HBPAE/$LiClO_4$) in the following section. The syntheses of $AB_2$ monomer and $SiO_2$-g-HBPAE/HBPAE composites were totally characterized. Meanwhile, the effects of the hypergrafting modification of nano-silica, nano-filler loading content and lithium salt dosage on the properties of composite polymer electrolytes were investigated. Comparing to traditional polymer electrolytes study, this work is hoped to provide a method for preparing solid-state polymer electrolytes with high ionic conductivity and good mechanical property.

## Experimental

### Materials and reagents

Lithium perchlorate ($LiClO_4$) (Alfa Aesar, USA) was dried under vacuum at 120 °C and reserved in a nitrogen-filled glove box (Etelux Lab2000). Fumed nano-silica (Aerosil 380) with an average primary particle size of 7 nm was supplied by Degussa Co., Germany. MMA, diethanolamine (DEA) (Alfa Aesar, USA) and APTES (Aladdin Co., China) were used as received. Toluene and acetonitrile was refluxed over calcium hydride for 12 h and then distilled under nitrogen before use.

### Preparation of samples

**Surface treatment of nano-silica** The nano-silica was dried at 110 °C under vacuum for 48 h before use. The mixture of 10.0 g nano-silica, 20.0 g APTES and 400 ml toluene was ultrasonically vibrated for 15 min and then refluxed with stirring for 24 h. Then, the temperature of the mixture was lowered to 30 °C, and 18.1 g MMA with sodium ethanolate was added as a catalyst. The reaction was maintained at 40 °C for a week under $N_2$ atmosphere. Such pretreated silica was recovered by centrifugation, extracted by toluene in a Soxhlet apparatus for 24 h to remove excess APTES coupling agent and MMA and finally dried under vacuum at 40 °C for 48 h, then at 100 °C for 12 h. Thus, reactive groups were introduced onto the surface of the nano-particles (for the convenience of discussion, the pretreated nano-silica was denoted as $SiO_2$-APTES-MMA in the following section). The amount of the coupling agent attached to nano-silica surface is 19.2 wt% as convinced by TGA measurement.

**The synthesis of $AB_2$ monomer** $AB_2$ monomer was synthesized by MMA and DEA through Michael addition reaction. The molar ratio of two reactants was 1.1:1.0 (MMA:DEA). Sodium ethoxide of 0.5 wt% was used as catalyst. The reaction was kept at 40 °C for a week under $N_2$ atmosphere. Unreacted substance was removed from the system under reduced pressure at 60 °C on a rotary evaporator.

**Polymerization and hypergrafting** The hyperbranched polymer was prepared as follows (Scheme 1): Firstly, a certain amount of $SiO_2$-APTES-MMA and $AB_2$ monomer (the proportion of $SiO_2$-APTES-MMA was separately 0, 5, 10, 15, 20 and 25 wt%) was added into the four-necked flask equipped with a thermometer, a blender and a condenser. Under vigorous agitating and reduced vacuum, the mixture was kept at 60 °C for 1 h, 80 °C for 1 h, 100 °C for 2 h and 120 °C for 4 h. Then, a certain amount of $LiClO_4$ dissolved in acetonitrile was added to the mixture to form a viscous solution. Finally, the blending solution was poured into silicone rubber mold,

**Scheme. 1** The synthesis of hyperbranched nano-silica

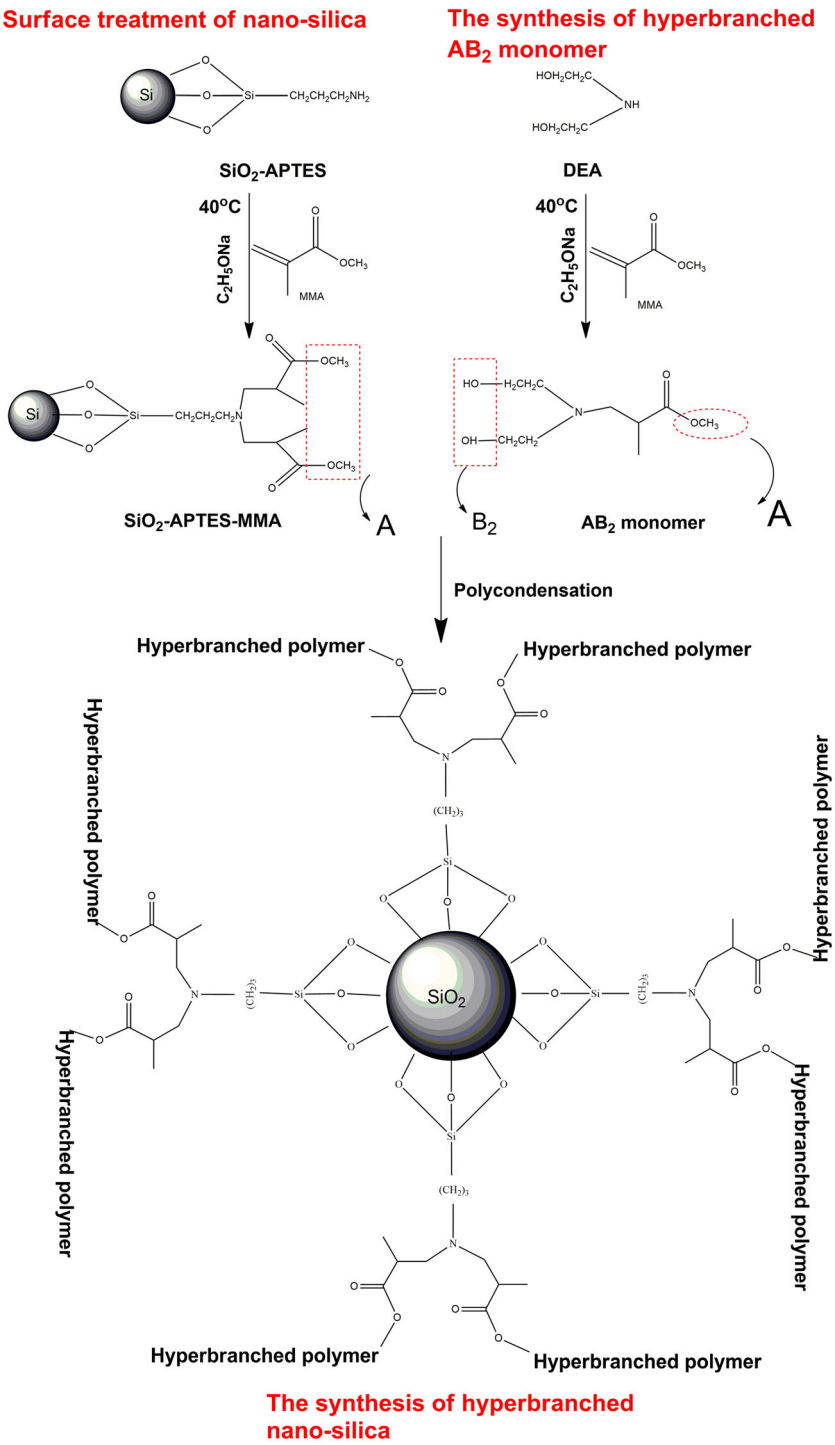


evaporated and dried in vacuum at 50 °C for 24 h to prepare composite polymer electrolytes (CPEs).

## Characterization of samples

The synthesis of $AB_2$ monomer and $SiO_2$-g-HBPAE/HBPAE was traced by fluorescence spectrometry (FS, VARIAN/Cary Eclipse). The nano-silica grafting ratio and thermal stability of the composite polymer electrolytes were determined by a Netzsch TG 209 thermo gravimetric analyzer (TGA) in nitrogen with a heating rate of 20 °C/min. The effect of nano-filler on the glass transition temperature (*Tg*) was tested by differential scanning calorimetry (DSC, TA/Q10). Transmission electron microscopy (TEM, Jeol/JEM-2010HR) and static light scattering (SLS, Brooken Haven/BI-200SM) were applied to look into the size of $SiO_2$-g-HBPAE and the

dispersion of $SiO_2$-g-HBPAE in DMF solution and HBPAE host. Rheological tests studied the content of $SiO_2$-APTES-MMA on the CPEs' mechanical properties. Gel permeation chromatography (GPC) was used to characterize molecular weight of polymer HBPAE.

The ionic conductivities of the CPEs were measured by Broadband dielectric spectrometer (Dielectric spectrometer, Triton technology). The electrolyte membranes with a thickness ranged from 100 to 200 μm were sandwiched between two platinum-plated parallel electrodes. The electrodes have a diameter of 20 mm fixed by electrode clamping block in a chamber. The temperature can be controlled with an accuracy ±0.1 °C with liquid nitrogen. All tests were carried out at the amplitude of 1.0 V under a dry inert atmosphere. The lithium-ion transference number of the sample was measured by chronoamperometry and impedance measurements in electrochemical workstation (IM6e, Zahner Zennium, Germany).

## Results and discussion

### The synthesis of $SiO_2$-g-HBPAE/HBPAE

Previous study has shown that the tertiary nitrogen can be excited to Rydberg state under UV irradiation and then emits fluorescence [32]. But for a low molecule tertiary amine compound, fluorescence is usually not observed due to the excited state being sensitive to the environment and the fluorescence quenching by intermolecular collisions. A tertiary amine has been produced during the preparation of $AB_2$ monomer through the Michael addition reaction between MMA and DEA. At the same time, a relatively large steric hindrance group was introduced, which could reduce the extent of fluorescence quenching. So fluorescence spectrum can be used to trace the synthesis of $AB_2$ monomer. Fluorescence intensity displayed in Fig. 1a increased along with the reaction time indicated that $AB_2$ monomer was successfully prepared.

The molecule weight of products increases along with the reaction time during the tri-functional $AB_2$ monomer polycondensation process. So it was essential to control the reaction time to avoid gelation occurrence. But it was difficult to study the kinetics of $AB_2$ monomer polymerization due to the lack of efficient characterization method. Yu studied the effects of reaction time on the polymerization by testing the degree of branch and molecular weight to optimize the reaction time [33]. This process was cumbersome and lengthy. In this work, fluorescence spectra were applied to characterize the hyperbranched condensation reaction process. The tertiary nitrogen was located in the polymer chain as branched units in hyperbranched (amine-ester), which could reduce the collision between tertiary nitrogen. The molecular weight

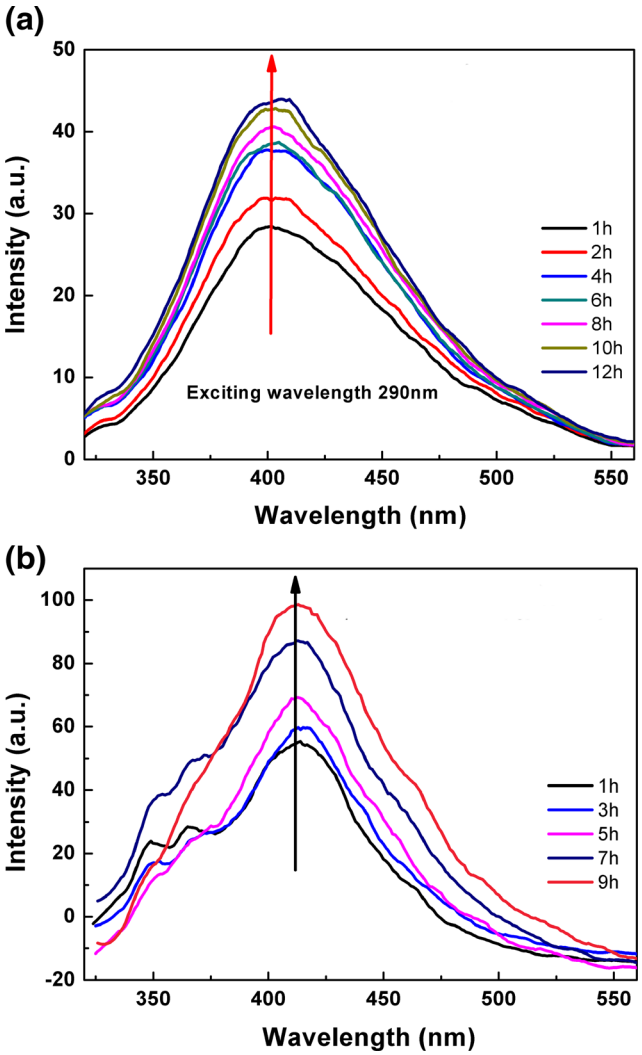


**Fig. 1** **a** The fluorescence spectra of synthetic monomer during reaction time. All the samples were dissolved in ultra-pure water at a concentration of 0.008 g/ml. **b** The fluorescence spectra of synthetic HBPAE during reaction time. All the samples were dissolved in *N,N*-dimethylformamide (DMF) at concentration of 0.008 g/ml

increased, and the movement of the polymer chain was slowed down along with reaction time, so the fluorescence intensity of the product became strong progressively. Therefore, the fluorescence spectra can be also used to track $AB_2$ monomer polymerization. As shown in Fig. 1b, the fluorescence intensity was equal to monomer at 60 °C (1 h) when the system did not initiate the polymerization. But when the temperature was rising to 80 °C (2–3 h), increasing fluorescence intensity indicated the $AB_2$ monomer was starting to polymerize. When the temperature was set up to 120 °C (6–9 h), the polymerization reaction accelerated, and the apparent viscosity together with fluorescence intensity increased significantly. After 3 h polycondensation, the fluorescence intensity tended to remain unchanged, which meant the attainment of equilibrium.

Hence, subsequent hyperbranched grafting process was carried out under this condition.

## The characterization of $SiO_2$-g-HBPAE/HBPAE

### *The dispersion and distribution of $SiO_2$-g-HBPAE*

The TEM images of hypergrafted nano-silica ($SiO_2$-g-HBPAE) with different loading of $SiO_2$-APTES-MMA (0~25 wt%) were displayed in Fig. 2. Figure 2a exhibits the morphology of HBPAE without incorporation of nano-silica. The loading of $SiO_2$-APTES-MMA when synthesizing $SiO_2$-g-HBPAE/HBPAE played an important role in the nano-silica dispersion (Fig. 2b-f). The results show that the incorporation of HBPAE could prevent nano-silica from self-aggregation. The corona with $SiO_2$ as cores ($SiO_2$-g-HBPAE) has been estimated to be an average thickness of 10~50 nm at the loading of 5~10 wt% of modified nano-silica (Fig. 2b-c). As the loading of nano-silica is higher, the dispersion state of $SiO_2$-g-HBPAE becomes poorer. Furthermore, the SLS results in Fig. 3 show that the average diameter of $SiO_2$-g-HBPAE in DMF solution ranged from 180 to 320 nm depending on the content of nano-silica loading during the synthesization of *$SiO_2$-g-HBPAE*. The less nano-silica loading, the larger corona obtained.

### *The grafting ratio of hypergrafted nano-silica*

For the hypergrafted nano-silica, two characteristic decomposition temperature stages of TGA curves can be observed, which are assigned to the decomposition of the terminal groups ($T_1$~200 °C) and polymer chains ($T_2$~400 °C), respectively (see supporting information Fig. S1). The grafting ratio of the hypergrafted nano-silica was estimated by the total weight loss of samples at 700 °C. In Fig. 4, the $T_1$, $T_2$ and grafting ratio are plotted against the loading of $SiO_2$-APTES-MMA. The values of $T_1$ of hypergrafted nano-silica are almost unchanged, which is ascribed to the decomposition of hydroxyl groups, while those of $T_2$ are slightly increased at higher loading benefited from the nano inclusions. When the loading of modified nano-silica was 15 wt%, the highest grafting ratio of the hypergrafted nano-silica reaches 283.1 %.

### *The DSC characterization of $SiO_2$-g-HBPAE/HBPAE*

As mentioned in the "Introduction" section, lowering glass transition temperature and increasing the polymer chains mobility are effective methods to improve ionic conductivities. Many studies indicated that segmental motion of the polymer chains was an essential element to design new polymer electrolyte [8–16]. So it is necessary to investigate the influencing factor on glass transition temperature ($T_g$) of the $SiO_2$-g-HBPAE/HBPAE. As shown in Fig. 5, the $T_g$ of specimen shifted significantly from 38.4 to −51.9 °C when loading 5 wt% $SiO_2$-APTES-MMA. But when an excess amount of nano-particles was added, the $T_g$ value increased along with $SiO_2$-APTES-MMA doping content. This change can be interpreted by hydrogen bond and nano-filler effect in composites. A large number of hydrogen bonds can be formed between HBPAE homopolymer due to the terminal hydroxyl.

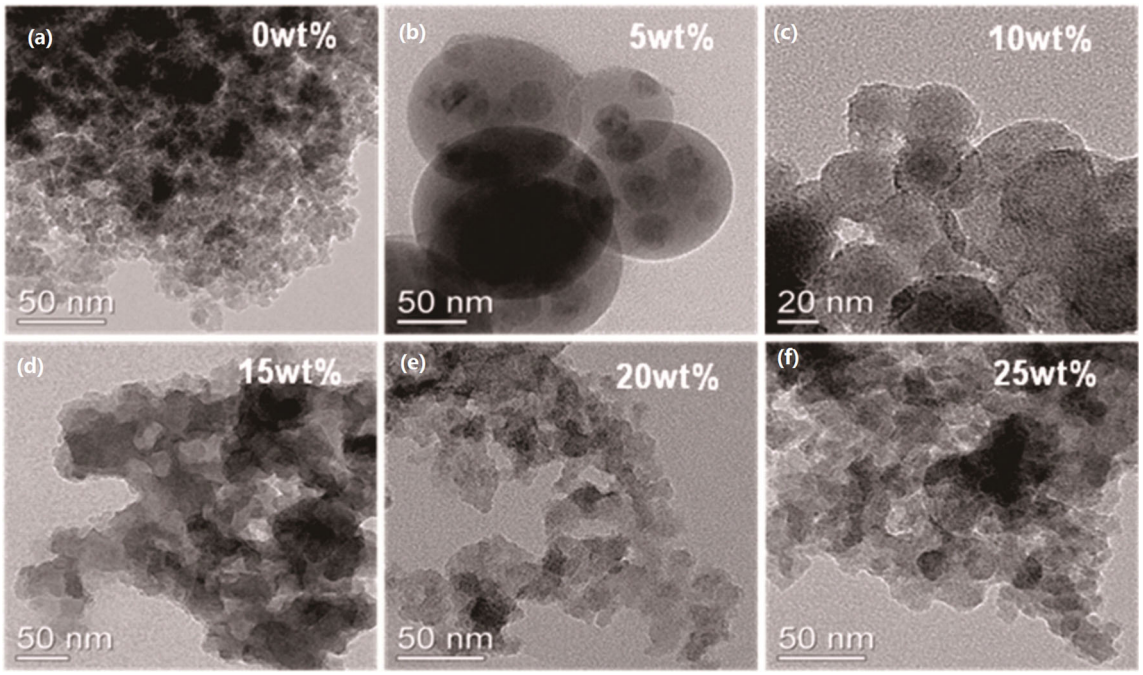


**Fig. 2** Dispersion of $SiO_2$-g-HBPAE with different $SiO_2$-APTES-MMA loading

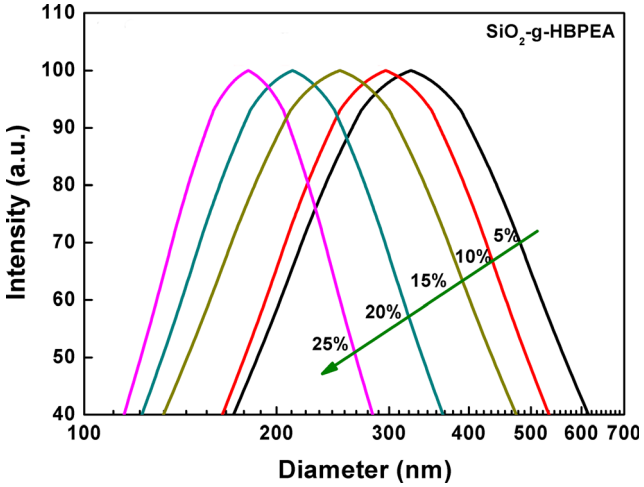


**Fig. 3** The diameters of $SiO_2$-g-HBPAE particles with different loading of $SiO_2$-APTES-MMA measured by SLS. The samples were dissolved in *N,N*-dimethylformamide (DMF) at a concentration of 0.001 g/ml and tested at 25 °C

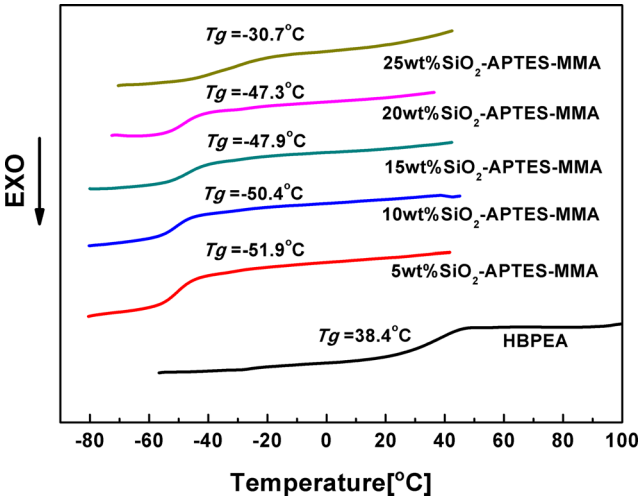


**Fig. 5** The DSC characterization of $SiO_2$-g-HBPAE/HBPAE composites with different $SiO_2$–APTES-MMA loading, DSC experiment was carried out with a rate of 5 °C/min in $N_2$ atmosphere

This strong interaction between molecules strengthened the polymer chain entanglement and obstructed the segmental movement, leading to a high glass transition temperature. Also bearing plenty of hydroxyl groups on the surface of $SiO_2$-g-HBPAE, when it incorporated to the HBPAE host, it could work as a solid plasticizer, just like multi-hydroxyl small molecule plasticizers, interacting with HBPAE hydroxyl groups and weakening HBPAE intermolecular interaction or even breaking the intermolecular hydrogen bonds [31]. These interaction changes in HBPAE host could promote the glass transition temperature shift to lower zone, as shown in Fig. 5.

The $T_g$ shifted to high value along with the increasing hypergrafted nano-silica contents when it exceeds 5 wt%, and this was a general trend of the effect of the nano-fillers on the $T_g$ of composites. Too much nanoparticle loading content in $SiO_2$-g-HBPAE/HBPAE composites may hinder the movement of polymer chains. It is noted that $SiO_2$-g-HBPAE with a grafting ratio of 283.1 % has the highest $T_g$ of −17.2 °C (see supporting information Fig. S2).

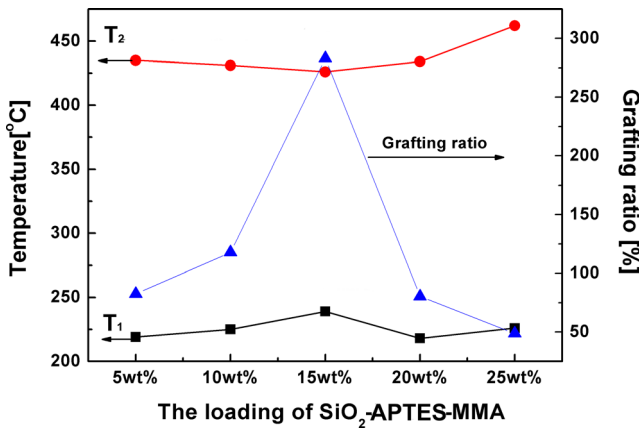


**Fig. 4** The effect of $SiO_2$-APTES-MMA on the decomposition temperature and grafting ratio. TGA experiment was carried out with a rate of 20 °C/min in $N_2$ atmosphere

*The rheological behaviour of $SiO_2$-g-HBPAE/HBPAE*

The incorporation of hypergrafted nano-silica into HBPAE could increase the rheological properties. In the frequency sweep mode of samples, the elastic shear modulus ($G'$) and viscous shear modulus ($G'$) of the composites are almost the constant at the small strain amplitude and dropped when stain amplitude exceeds a certain threshold value (see supporting information Fig. S3). The $G'$ and $G''$ of HBPAE are significantly improved with the loading of $SiO_2$-APTES-MMA. The hypergrafted nano-silica can act as reinforcing phase due to its inherent strength and good interface compatibility with the HBPAE matrix. With the increase of nano-filler loading, the friction among nano-fillers would also increase. The composite with 10 wt% of $SiO_2$-APTES-MMA inclusions exhibits the highest modules of $G'$ and $G''$, with the grafting ratio of almost 117.8 % for the nano-silica. However, the inorganic fillers slightly deteriorate the deformation rate of the samples with a smaller strain threshold value. Too much addition of nano-inclusion may be highly aggregative, which causes the failure of nano-filler effect.

## The electrochemical properties of $SiO_2$-g-HBPAE/HBPAE CPEs

The ionic conductivities of $SiO_2$-g-HBPAE/HBPAE CPEs with different loading of $SiO_2$-g-HBPAE and $LiClO_4$ were investigated at a temperature range from 20 to 100 °C. In the following experiments, 100 KHz was taken to measure the ionic conductivity ($\sigma$) of CPEs for comparison according to our previous work [31].

In order to study the influence of $SiO_2$-g-HBPAE on the $\sigma$ of CPEs, a series of samples were made with 30 wt% $LiClO_4$ doped. The obtained $\sigma$ variation of the different loading of nano-silica feeding as a function of temperature reciprocal is shown in Fig. 6a. It was noticeable that the ionic conductivity improved progressively with the addition of $SiO_2$-APTES-MMA compared to HBPAE host at low loading. When the loading of fillers reached a content of 10 wt%, the specimen gained the maximum value of ionic conductivity at testing temperature. The glass transition temperature was shifted to high temperature along with the $SiO_2$-APTES-MMA loading, which was unfavourable for ionic transportation. This is why the ionic conductivity decreased when $SiO_2$-APTES-MMA content exceeding 10 wt%. Meanwhile, as the molecule of HBPAE was about 2000 according to the GPC result, the interaction between HBPAE chains was too weak to afford good mechanical property without nano-silica particles. Hence, a proper loading content has to be optimized to gain both high ionic conductivity and good mechanical property. A weight percent of 10 was considered to be an optimized value according to the dielectric and rheology results.

It also can be seen from the plots that the temperature dependence of $\sigma$ shows approximate Arrhenius behaviour with slight deviation across the entire testing temperature. This is because ionic transport in CPEs appears to be occurred on the surface of the nano-particles or through a low-density polymer phase at the interface, decoupled from the polymer relaxation mechanisms, leading to an Arrhenius-type, almost straight-line plot [34–39]. But when in a hybrid system especially at a high nano-particle loading, some active plots of the nano-fillers were covered up due to the agglomeration, which might result in deviation from Arrhenius behaviour for CPEs. In this situation, Li-ions therefore would be able to move both via segmental motion of the polymer as well as by activated hops along the surface of the fillers [40].

Then, a series of specimens with different $LiClO_4$ doping contents were prepared under a fixed content of 10 wt% $SiO_2$-APTES-MMA. As shown in Fig. 6b, the ionic conductivity

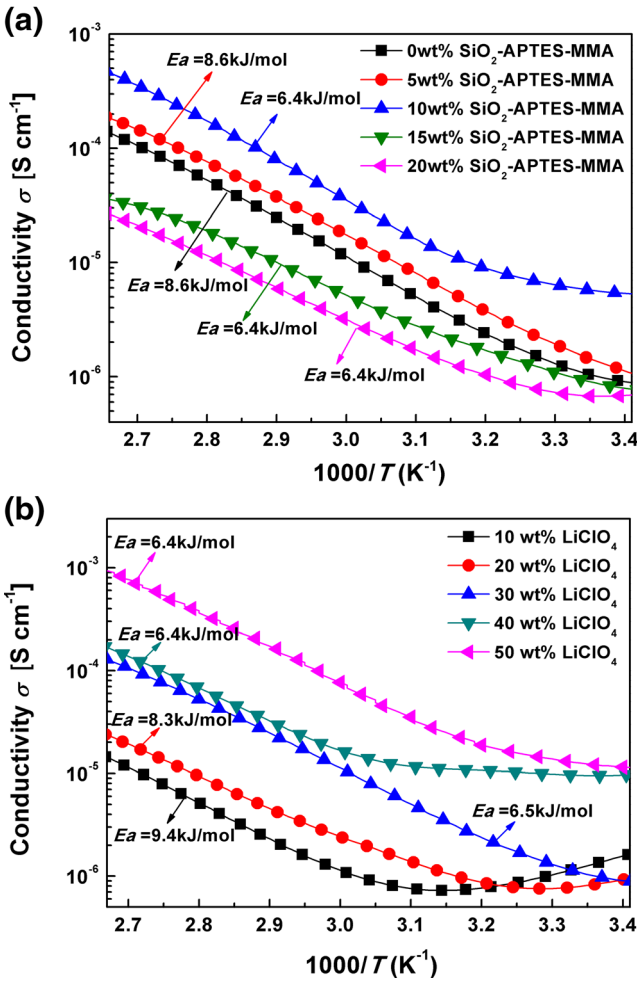


**Fig. 6** **a** The effect of $SiO_2$ loading on the ionic conductivity of $SiO_2$-g-HBPAE/HBPAE/$LiClO_4$ ($LiClO_4$ content: 30 wt%); **b** the effect of $LiClO_4$ content on the ionic conductivity of $SiO_2$-g-HBPAE/HBPAE/$LiClO_4$ (loading of 10 wt% $SiO_2$-APTES-MMA: 10 wt%)

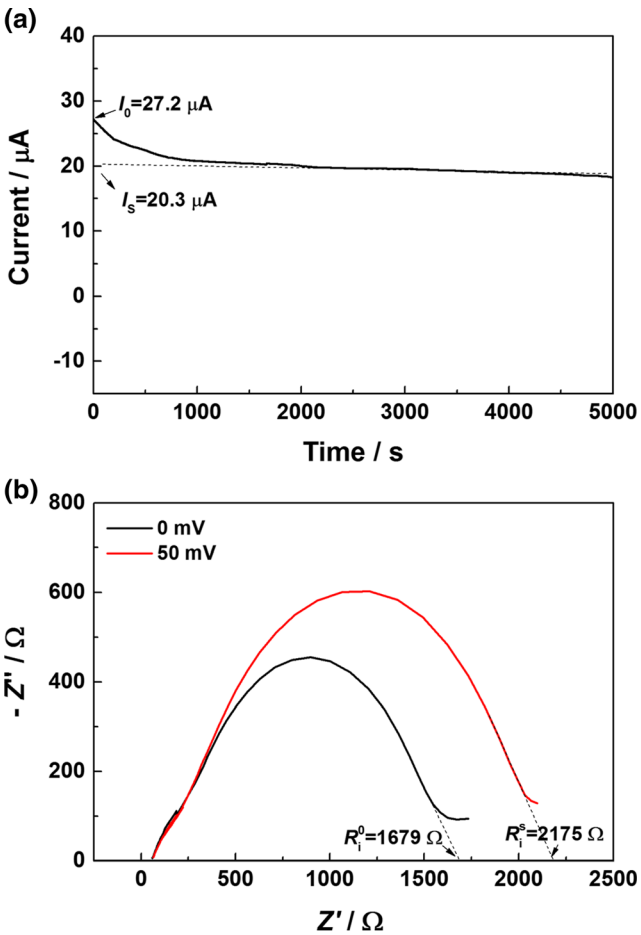


**Fig. 7** **a** Chronoamperometry curve for synthesized hyperbranched electrolyte assembled in metal lithium/polymer electrolyte/metal lithium cell; **b** electrochemical impedance spectra of metal lithium/polymer electrolyte/metal lithium cell at different potentials. Frequency range 10 mHz ~100 kHz

was significantly improved along with the $LiClO_4$ doping contents and testing temperature. However, the Arrhenius conductivity plot between conductivity and temperature was non-linear except 30 wt% $LiClO_4$. This indicates that neither electrolyte system exhibited Arrhenius-like behaviour. This phenomenon was also found in PEO-$LiSO_3CF_3$ polymer matrix incorporating nano-metric $Al_2O_3$ [41]. The non-Arrhenius-like behaviour was associated with dynamic temperature dependence restructuring of the anion "sub-lattice" [42] or the polymer segment relaxation [43]. The conductance performance of composite polymer electrolyte improved along with $LiClO_4$ doping content above 30 wt%. This is a general trend owing to the increasing number of charge carriers for electrolyte [44]. The non-Arrhenius behaviour indicated that a comparative ability to decouple ion transport from motions of the polymer host was also gained in such CPEs. This affect might be attributed to the hypergrafted surface modification. The hyperbranched poly (amine-ester) grafting to the nano-silica has a cavity structure, which may offer an ionic conducting channel along the interphase.

The Vogel-Tamman-Fulcher (VTF) equation was used to fit the non-Arrhenius behaviour. The equation is shown as follows:

$$\sigma = \sigma_0 T^{-1/2} exp^{-Ea/R\ (T,-,Tg)} \quad (1)$$

Where $\sigma_0$ is the pre-exponential factor, $T$ is the absolute temperature, $E_a$ is the activation energy (kJ/mol), $R$ is the gas constant, ~8.314 J/(K·mol) and $T_g$ is the glass transition temperature. The calculated $E_a$ is also marked in Fig. 6. It is shown in Fig. 6b that with 10 wt% of hypergrafted nano-silica, the $SiO_2$-g-HBPAE/HBPAE/30 wt% $LiClO_4$ composite electrolyte has the best ionic conductivity probably due to its low activation energy (6.4 kJ/mol). When the $LiClO_4$ doping content reached 50 wt%, the conductivity was dramatically enhanced, a promising conductivity of about $1.4\times10^{-5}$ S/cm at room temperature.

The transference number ($t_+$) of synthesized hyperbranched electrolyte of this optimized CPE was measured in a simulated battery by an assembly of metal lithium/polymer electrolyte/metal lithium together. The value of $t_+$ is calculated according to the formula (2) as follows:

$$t_+ = \frac{I_S\left(\Delta V - I_O R_i^O\right)}{I_O\left(\Delta V - I_S R_I^S\right)'} \quad (2)$$

where $I_0$ is the initial current; $\Delta V$ is the applied potential, $AV = 50mV$ $I_s$ is the steady-state current; $R_i^O$ and $R_I^S$ are the electrode resistance before and after the potentiostatic polarization, respectively. The parameters of $I_0$, $I_s$, $R_i^O$ and $R_I^S$ are determined by chronoamperometry and impedance measurements, as shown in Fig. 7. The calculated $t_+$ of synthesized hyperbranched electrolyte of this optimized CPE reaches about ~0.55. The high value of $t_+$ is probably due to the interaction between hyperbranched structure (oxygen and nitrogen contained) and anion ($ClO_4^-$) of dissociated lithium salt. The strong interaction can greatly slow down the transportation of $ClO_4^-$ so that the movement of lithium ions within the solid electrolyte is preferred [45].

## Conclusion

In summary, a solid-state polymer electrolyte of hyperbranched nano-composites of $SiO_2$-g-HBPAE/HBPAE/$LiClO_4$ was prepared. The fluorescence spectra were used to trace the synthesization procedure of composite electrolytes. The dispersed size and grafting ratio of hypergrafted nano-silica were measured. The effect of such silica on the motion of polymer chains and mechanical properties of HBPAE was characterized. The conductivity of $SiO_2$-g-HBPAE/HBPAE/$LiClO_4$ with 10 wt% nano-inclusions and 50 wt% $LiClO_4$ could reach the best of $1.4\times10^{-5}$ S/cm at 30 °C and ~$10^{-3}$ S/cm at 100 °C. Additionally, the transference number of synthesized hyperbranched electrolyte can be up to 0.55. This type of composite electrolyte has a potential application in polymer lithium batteries in order to solve the liquid electrolyte leakage and security problems.

**Acknowledgment** The authors would like to acknowledge the financial support from Natural Science Foundation of China (Grant: 51473186, 51173207, U1201243), the Natural Science Foundation of Guangdong, China (Grants: 2013B010135001 2012A090100006, 2012B091000065, the Science and Technology Planning Project of Guangdong, China (Grants: 2013B010204023).

## References

1. Wakihara M, Kadoma Y, Kumagai N, Mita H, Araki R, Ozawa K, Ozawa Y (2012) Development of nonflammable lithium ion battery using a new all-solid polymer electrolyte. J Solid State Electrochem 16:847–855
2. Shintani Y, Tsutsumi H (2010) Ionic conducting behavior of solvent-free polymer electrolytes prepared from oxetane derivative with nitrile group. J Power Sources 195:2863–2869
3. Ramesh S, Wong KC (2009) Conductivity, dielectric behaviour and thermal stability studies of lithium ion dissociation in poly(methyl methacrylate)-based gel polymer electrolytes. Ionics 15:249–254
4. Lee JY, Lee YM, Bhattacharya B, Nho Y-C, Park J-K (2010) Solid polymer electrolytes based on crosslinkable polyoctahedral silsesquioxanes (POSS) for room temperature lithium polymer batteries. J Solid State Electrochem 14:1445–1449
5. Lee JI, Kim DW, Lee C, Kang Y (2010) Enhanced ionic conductivity of intrinsic solid polymer electrolytes using multi-armed oligo(ethylene oxide) plasticizers. J Power Sources 195:6138–6142
6. Yarmolenko OV, Khatmullina KG, Tulibaeva GZ, Bogdanova LM, Shestakov AF (2012) Towards the mechanism of $Li^+$ ion transfer in the net solid polymer electrolyte based on polyethylene glycol diacrylate–$LiClO_4$. J Solid State Electrochem 16:3371–3381

7. Kelly IE, Owen JR, Steele BCH (1985) Poly(ethylene oxide) electrolytes for operation at near room temperature. J Power Sources 14:13–21
8. Beata K (2014) Precipitated silica as filler for polymer electrolyte based on poly(acrylonitrile)/sulfolane. J Solid State Electrochem 18:2035–2046
9. Oh JS, Kim SH, Kang Y, Kim DW (2006) Electrochemical characterization of blend polymer electrolytes based on poly(oligo[oxyethylene]oxyterephthaloyl) for rechargeable lithium metal polymer batteries. J Power Sources 163:229–233
10. Chiu CY, Chen HW, Kuo SW, Huang CF, Chang FC (2004) Investigating the effect of miscibility on the ionic conductivity of $LiC1O_4$/PEO/PCL ternary blends. Macromolecules 37:8424–8430
11. Rocco AM, Da Fonseca CP, Pereira RP (2002) A polymeric solid electrolyte based on a binary blend of poly(ethylene oxide), poly(methyl vinyl ether-malefic acid) and $LiClO_4$. Polymer 43: 3601–3609
12. Gomez ED, Panday A, Feng EH, Chen V, Stone GM, Minor AM, Kisielowski C, Downing KH, Borodin O, Smith GD, Balsara NP (2009) Effect of ion distribution on conductivity of block copolymer electrolytes. Nano Lett 9:1212–1216
13. Zhang YG, Zhao Y, Bakenov Z, Gosselink D, Chen P (2014) Poly(vinylidene fluoride-co-hexafluoropropylene)/poly(methylmethacrylate)/nanoclay composite gel polymer electrolyte for lithium/sulfur batteries. J Solid State Electrochem 18:1111–1116
14. Singly M, Odusanya O, Wilmes GM, Eitouni HB, Gomez ED, Patel AJ, Chen VL, Park MJ, Fragouli P, Iatrou H, Hadjichristidis N, Cookson D, Balsara NP (2007) Effect of molecular weight on the mechanical and electrical properties of block copolymer electrolytes. Macromolecules 40:4578–4585
15. Panday A, Mullin S, Gomez ED, Wanakule N, Chen VL, Hexemer A, Pople J, Balsara NP (2009) Effect of molecular weight and salt concentration on conductivity of block copolymer electrolytes. Macromolecules 42:4632–4637
16. Young WS, Epps TH (2009) Salt doping in PEO-containing block copolymers: counterion and concentration effects. Macromolecules 42:2672–2678
17. Liang YH, Cheng-Chien WB, Chen CY (2008) Comb-like copolymer-based gel polymer electrolytes for lithium ion conductors. J Power Sources 176:340–346
18. Zheng JY, Li X, Yu YJ, Zhen XM, Song YY, Feng XM, Zhao YF (2014) Cross-linking copolymers of acrylates' gel electrolytes with high conductivity for lithium-ion batteries. J Solid State Electrochem 18:2013–2018
19. Nishimoto A, Agehara K, Furuya N, Watanabe T, Watanabe M (1999) High ionic conductivity of polyether-based network polymer electrolytes with hyperbranched side chains. Macromolecules 32:1541–1548
20. Lee S, Schomer M, Peng HG, Page KA, Wilms D, Frey H, Soles CL, Yoon DY (2011) Correlations between ion conductivity and polymer dynamics in hyperbranched Poly(ethylene oxide) electrolytes forlithium-ion batteries. Chem Mater 23:2685–2688
21. Itoh T, Ichikawa Y, Hirata N, Uno T, Kubo M, Yamamoto O (2002) Effect of branching in base polymer on ionic conductivity in hyperbranched polymer electrolytes. Solid State Ion 150:337–345
22. Itoh T, Ichikawa Y, Uno T, Kubo M, Yamamoto O (2003) Composite polymer electrolytes based on poly(ethylene oxide), hyperbranched polymer, $BaTiO_3$ and $LiN(CF_3SO_2)_2$. Solid State Ion 156:393–399
23. Ye L, Gao P, Zhao YM, Feng ZG, Bai Y, Wu F (2008) Preparation and evaluation of two kinds of solid polymer electrolytes made from crosslinked poly(ether urethane) elastomers consisting of a comb-like and a hyperbranched polyether. J Appl Polym Sci 109: 1955–1961
24. Deka M, Kumar A, Deka H, Karak N (2012) Ionic transport studies in hyperbranched polyurethane/clay nanocomposite gel polymer electrolytes. Ionics 18:181–187
25. Wu C, Wu F, Bai Y, Feng T, Pan CH, Ye L, Feng ZG (2009) Preparation and characteristics of novel hyperbranched PEU-based gel polymer electrolytes. J Chil Cheml Soc 54:299–301
26. Pan YC, Diganta S, Jason F, Tsaib LD, Feyc GTK, Kao HM (2011) Synthesis and characterization of a new hyperbranched organic–inorganic solid polymer electrolyte with cyanuric chloride as a core element. Electrochim Acta 56:8519–8529
27. Manuel Stephan A, Nahm KS, Anbu Kulandainathan M, Ravi G, Wilson J (2006) Electrochemical studies on nanofiller incorporated poly(vinylidene fluoride–hexafluoropropylene) (PVdF–HFP) composite electrolytes for lithium batteries. J Appl Electrochem 36: 1091–1097
28. Fahmi EM, Ahmad A, Rahman MYA, Hamzah H (2012) Effect of NiO nanofiller concentration on the properties of PEO-NiO-$LiClO_4$ composite polymer electrolyte. J Solid State Electrochem 16:2487–2491
29. Low SP, Ahmad A, Hamzah H, Rahman MYA (2010) Nanocomposite solid polymeric electrolyte of 49% poly(methyl methacrylate)-grafted natural rubber–titanium dioxide–lithium tetrafluoroborate (MG49-$TiO_2$-$LiBF_4$). J Solid State Electrochem 15:2611–2618
30. Rao MM, Liu JS, Li WS, Liao YH, Liang Y, Zhao LZ (2009) Polyethylene-supported poly(acrylonitrile-co-methyl methacrylate)/nano-$Al_2O_3$ microporous composite polymer electrolyte for lithium ion battery. J Solid State Electrochem 14: 255–261
31. Hu XL, Hou GM, Zhang MQ, Rong MZ, Ruan WH, Emmanuel PG (2012) A new nanocomposite polymer electrolyte based on poly(-vinyl alcohol) incorporating hypergrafted nano-silica. J Mater Chem 22:18961–18967
32. Yang W, Pan CY (2009) Synthesis and fluorescent properties of biodegradable hyperbranched poly (amido amine)s. Macromol Rapid Comm 30:2096–3001
33. Yu Y, Rong MZ, Zhang MQ (2010) Grafting of hyperbranched aromatic polyamide onto silica nanoparticles. Polymer 51:492–499
34. Croce F, Appetecchi GB, Persi L, Scrosati B (1998) Nanocomposite polymer electrolytes for lithium batteries. Nature 394:456–458
35. Nugent JL, Moganty SS, Archer LA (2010) Nanoscale organic hybrid electrolytes. Adv Mater 22:3677–3680
36. Aydın H, Şenel M, Erdemi H (2011) Inorganic–organic polymer electrolytes based on poly(vinyl alcohol) and borane/poly(ethylene glycol) monomethyl ether for Li-ion batteries. J Power Sources 196: 1425–1432
37. Malathi J, Kumaravadivel M, Brahmanandhan GM, Hema M, Baskaran R, Selvasekarapandian S (2010) Structural, thermal and electrical properties of PVA–LiCF3SO3 polymer electrolyte. J Non-Cryst Solids 356:2277–2281
38. Rajendran S, Sivakumar M, Subadevi R, Wu NL, Lee JY (2007) Electrochemical investigations on the effect of dispersoid in PVA based solid polymer electrolytes. J Appl Polym Sci 103:3950–3956
39. Jacob MME, Hackett E, Giannelis EP (2003) From nanocomposite to nanogel polymer electrolytes. J Mater Chem 13:1–5
40. Adebahr J, Best AS, Byrne N, Jacobsson P, MacFarlane DR, Forsyth M (2003) Ion transport in polymer electrolytes containing nanoparticulate $TiO_2$: the influence of polymer morphology. Phys Chem Chem Phys 5:720–725
41. Croce F, Persi L, Scrosati B, Serraino-Fiory F, Plichta E, Hendrickson MA (2001) Role of the ceramic fillers in enhancing the transport properties of composite polymer electrolytes. Electrochim Acta 46:2457–2461
42. Kincs J, Martin SW (1996) Non-arrhenius conductivity in glass: mobility and conductivity saturation effects. Phys Rev Lett 76:70–73

43. Su'ait MS, Ahmad A, Hamzah H, Rahman MYA (2011) Effect of lithium salt concentrations on blended 49% poly(methyl methacrylate) grafted natural rubber and poly(methyl methacrylate) based solid polymer electrolyte. Electrochim Acta 57: 123–131
44. Lavall RL, Ferrari S, Tomasi C, Marzantowicz M, Quartarone E, Magistris A, Mustarelli P, Lazzaroni S, Fagnoni M (2010) Novel polymer electrolytes based on thermoplastic polyurethane and ionic liquid/lithium bis(trifluoromethanesulfonyl) imide/propylene carbonate salt system. J Power Sources 195:5761–5767
45. Kato Y, Yokoyama S, Yabe T, Ikuta H, Uchimoto Y, Wakihara M (2004) Ionic conductivity and transport number of lithium ion in polymer electrolytes containing PEG–borate ester. Electrochim Acta 50:281–284